

A Computational Study of the Crystal and Electronic Structure of the Room Temperature Organometallic Ferromagnet $V(TCNE)_2$

ANDERIL TCHOUGRÉEFF,¹ RICHARD DRONSKOWSKI²

¹Division of Electrochemistry, Department of Chemistry, MSU Moscow, Russia

²Institute of Inorganic Chemistry, RWTH Aachen, D-52056 Aachen, Germany

Received 4 January 2008; Accepted 29 February 2008

DOI 10.1002/jcc.20987

Published online 1 May 2008 in Wiley InterScience (www.interscience.wiley.com).

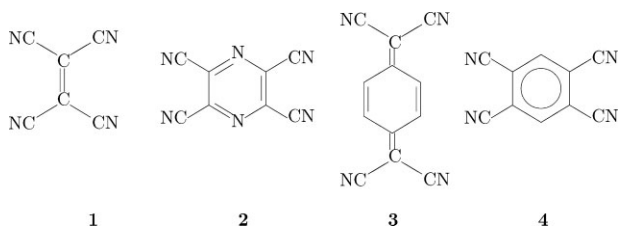
Abstract: We study numerically the crystal and electronic structure of the room temperature organometallic ferromagnet of general composition $V(TCNE)_x \times y$ solvent with $x \approx 2$, starting from both the experimental structure of its iron analog which results from the EXAFS experiment as well as the theoretical model structure compatible with magnetic measurements on this type of compounds. The results of the numerical study performed at the density functional level of theory show that the experimentally determined structure complies with the magnetic measurements and thus can serve as a prototype structure for the entire family of the $M(TCNE)_2$ organometallic magnets. Both the results of the numerical study and the magnetic experiments are interpreted using a proposed model Hamiltonian.

© 2008 Wiley Periodicals, Inc. J Comput Chem 29: 2220–2233, 2008

Key words: organometallic magnets; numerical study; band model; spatial structure; electronic structure

Introduction

A room temperature organometallic ferromagnet of approximate composition $V(TCNE)_x \times y$ solvent (where TCNE – **1** – stands for tetracyanoethylene – a well known organic electron acceptor; $x \approx 2$ and y depends on the type of the solvent) supplied by about one half



of the solvent molecule CH_2Cl_2 per formula unit had been synthesized yet in the beginning of the 1990's¹ as an amorphous moisture sensitive precipitate. Its most remarkable property was the non-vanishing spontaneous magnetization persistent almost up to the decomposition temperature of about 350 K which allowed to estimate the critical temperature of the ferromagnetic transition (the Curie temperature) to be of about 400 K, that is, higher than the

decomposition temperature itself. The following years witnessed many analogs of the above compound both in terms of extending variety of involved organic acceptors (ref. 2 – tetracyanopyrazine – **2**; ref. 3 – 7,7,8,8-tetracyano-*p*-quinodimethane – **3**; ref. 4 – tetracyanobenzene – **4**) and in terms of the metals (ref. 5 – iron), although none of them manifested as fascinating magnetic properties as the first $V(TCNE)_2$ compound (the Curie temperatures ranged from 44 K for Ni and Co compounds through 107 K for the Mn to 121 K for the Fe compound – all with TCNE). Varying the solvent also affects the Curie temperature, e.g., replacement of CH_2Cl_2 presented in the original compound ref. 1 by tetrahydrofuran (THF) reduces the Curie temperature of $V(TCNE)_x \times y$ solvent to 210 K and by MeCN to about 100 K.

Generally one has to say that not only the Curie temperature, but also other properties of the compounds of the considered class are sensitive to the details of the preparation procedure. For example,

Correspondence to: A. L. Tchougréeff; e-mail: tch@elch.chem.msu.ru

Dedicated to Prof. R. Hoffmann on the occasion of his 70-th birthday

Contract/grant sponsor: RFBR; contract/grant numbers: 05-07-90067, 07-03-01128

Contract/grant sponsor: DFG(RWTH-Aachen University); contract/grant numbers: DR342/18-1

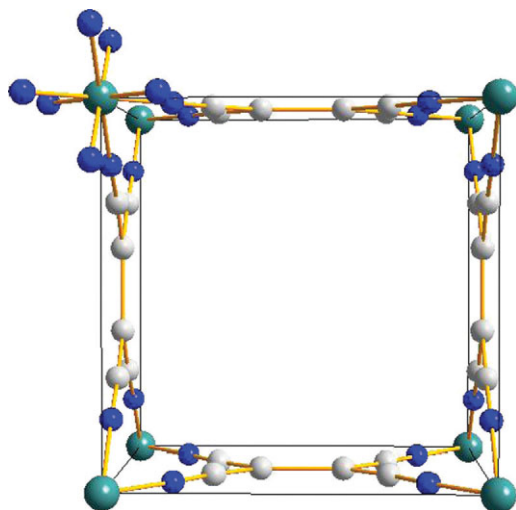
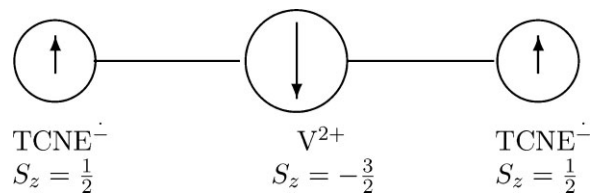


Figure 1. Hypothetical structure of $V(TCNE)_2$ following.⁶

the V-TCNE compound is known in two forms – the original of ref. 1 coming from the reaction of $V(C_6H_6)_2$ with TCNE and another obtained from vanadium hexacarbonyl $V(CO)_6$. The latter exhibits a magnetization that is almost twice as strong at the zero temperature compared to the original one.

For more than one decade the amorphousness of the compound of interest did not allow to make any definite conclusions concerning its structure so that the statement made in ref. 6 “almost nothing is known about the actual structure of the V-TCNE ferromagnet” remained true during these years. Nevertheless, the reasonable limitations upon the tentative structure could be formulated yet in ref. 6. These conditions are as follows. The acceptable structure has to (i) correspond to the observed composition $V(TCNE)_2$, (ii) form a three-dimensional network of V atoms and TCNE molecules without pronounced anisotropy to ensure the proliferation of the magnetic order through the sample, and (iii) be loose enough to be able to accommodate solvent molecules. These simple ideas allowed the authors of⁶ to propose a structure compatible with the magnetic data available at that time. It is presented in Fig. 1, where one can see rather spacious channels capable to accommodate solvent molecules. The V atoms experiences 8-fold coordination by the N atoms; the V–N distance being about 2.06 Å.

In the frame of that model it was possible to discuss the tentative electronic structure of the new material with the purpose to understand the most intriguing – the magnetic properties. It was assumed that two unpaired electrons occupy the LUMO $b_{3g}(\pi^*)$ -orbitals of the two TCNE units forming respective anion radicals $TCNE^{\dot{-}}$ and three more of them reside in the d -shell of the vanadium (II) cations acquiring there a high-spin configuration with the total spin 3/2. In contrast with the description of the $V(TCNE)_2$ compound as a “ferromagnet” the effective magnetic interaction between the local spins 1/2, 1/2, and 3/2 has an “antiferromagnetic” sign i.e. the spins 3/2 located on vanadium ions tend to be oriented in the opposite direction to that of the spins 1/2 located on the $TCNE^{\dot{-}}$ units, so that the spontaneous magnetic momentum corresponds to overall value of one unpaired electron per formula unit (or per vanadium atom):



This view was supported by the electronic structure model proposed in⁶ which is characterized by complete filling of involved bands by electrons of only one spin projection extensively used by other authors.⁷ The model⁶ represents an unrestricted Hartree–Fock (UHF) band model spanned by three d -orbitals of vanadium ions and two acceptor orbitals per unit cell of the hypothetical structure in Figure 1. The calculations with use of this model produce five very flat bands (in fact two of the three predominantly d - and one of the two predominantly acceptor bands have zero dispersion. These bands are strongly split into subbands corresponding to different projections of spins of electrons occupying these subbands which yields the model density of states (DoS) shown in Figure 2.

The fact that the bands obtained in the calculations are extremely narrow and the subbands corresponding to different projections of electron spins are completely filled indicates that the local description may be more adequate. It reduces to the Heisenberg Hamiltonian describing the interactions of the above local spins 1/2 and 3/2. The interactions are of the “antiferromagnetic” sign so that the interacting spins are aligned in the opposite directions.

The main objection against the model ref. 6 was the eight-fold coordination of the vanadium atom by nitrogen atoms coming from eight respective $TCNE^{\dot{-}}$ units, being in contrast with six-coordination which one would usually expect. The latter viewpoint found experimental support⁹ from the EXAFS and XANES experiments which have shown the average coordination number of vanadium to be 6.04 ± 0.25 and have strongly emphasized almost octahedral environment of the latter although have not been able to completely resolve the structure issues. The critical breakthrough came with the recent EXAFS work¹⁰ where the authors were able to establish the structure of the Fe^{2+} analog (presented in Fig. 3)

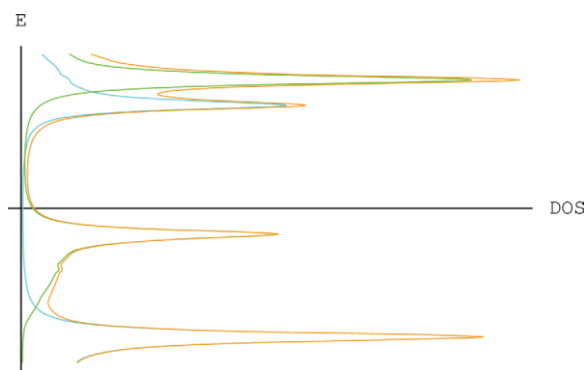


Figure 2. Model density of electronic states of $V(TCNE)_2$ (in red) in two spin channels (respectively green and blue) following.⁶ The occupied subbands spanned by the d -states and acceptor states respectively belong to the channels with opposite spin projections.

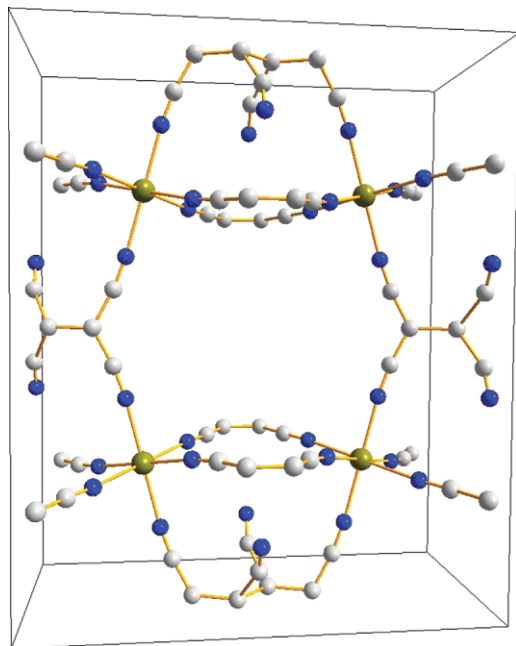


Figure 3. Structure of $\text{Fe}(\text{TCNE})_2$ as coming from the EXAFS study.¹⁰ Each unit cell contains four formula units. The solvent molecules are omitted for clarity.

of the $\text{V}(\text{TCNE})_2$ compound and revealed some of its remarkable features. It had been shown that the dimer form of the $\text{TCNE}^{\cdot-}$ radical-anion: $[\text{TCNE}]_2^{2-} = \text{C}_4(\text{CN})_8^{2-}$ plays an important role in shaping the loose three-dimensional structure satisfying the general

Table 1. Semiempirical Values of on Site Coulomb Repulsion Parameters for Involved Atoms to be Used in LSDA+ U Modeling.

	F^0 eV	F^2 eV
V	13.36	6.100
N	12.10	4.729
C	11.07	5.957

conditions of ref. 6 and that of the octahedral coordination of the metal ion.

Because of the existence of the dimer form of the $\text{TCNE}^{\cdot-}$ radical-anion with doubled charge, we note that the synthesis of a chemically even simpler class of magnetic materials containing bridging N atoms has recently been accomplished. The so called 3d carbodiimides incorporate divalent magnetic transition metal (e.g. Mn^{2+} , Fe^{2+} , Co^{2+} , and Ni^{2+}) that are connected to each other by the NCN^{2-} molecular anions, the basic form of carbodiimides (or cyanamide) molecule, forming a three-dimensional structure. In all cases the transition metal cations experience the octahedral coordination whereas the NCN^{2-} units may be also octahedrally coordinated (following the [NaCl] type such as in MnNCN compound¹²) or coordinated according to the motif of a trigonal prism (quasi [NiAs] or delafossite type as in $\text{CoNCN}/\text{NiNCN}$ ¹³). Antiferromagnetic coupling between the magnetic centers is characteristic for this novel class of compounds which may be looked upon as nitrogen-containing analogs of the 3d-metal oxides.

We see that the chemical composition of the “organic” part of the organic ferromagnet resembles that of the well-studied carbodiimides. Next, since the ionic radii of V^{2+} and Fe^{2+} almost coincide

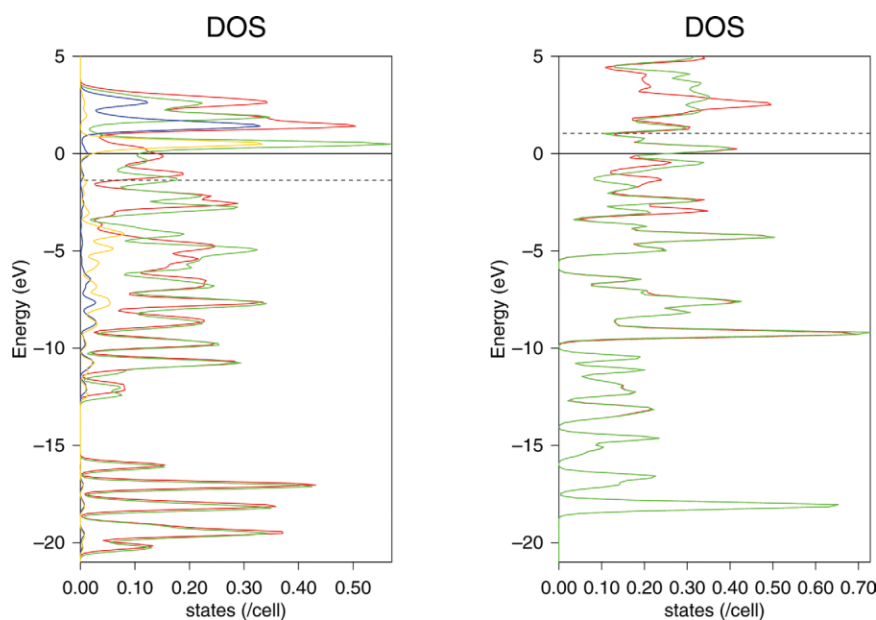


Figure 4. Densities of states in two spin channels for the compressed (left) and relaxed (right) structures of ref. 6. Spin projections of the total DoS are given respectively in green and red; and spin projections on the d-states of metal atoms in blue and yellow.

(respectively 0.79 and 0.78 Å for the high-spin form of Fe²⁺)¹¹ and also due to the fact that the solid solutions of the composition Fe_xV_{1-x}(TCNE)₂ in a wide range of *x* form readily it seems to be possible to use the structure¹⁰ (Fig. 3) as a starting point for further consideration.

Numerical Experiments

In the present work we continued our efforts directed to concert elucidation of the spatial and electronic structure of the room temperature organometallic ferro(ferri)magnet V(TCNE)₂. Close analogy with transition metal carbodiimides allows the use of the solid-state electronic-structure package VASP.¹⁴ We performed calculations on several structures which could be considered as relevant to the problem. The calculation had been performed with use of the LSDA+*U* functional where the *U* term had been added for the *d*-shells of vanadium ions and *p*-shells of carbon and nitrogen atoms to ensure the convergence of calculations to a spin-polarized ground state. The LSDA+*U* functional had been taken in the form:

$$E_{\text{LSDA}+U} = E_{\text{LSDA}} + U + \frac{(U - J)}{2} \times \sum_{\sigma} \left[\left(\sum_m n_{mm}^{\sigma} \right) - \left(\sum_{mm'} n_{mm'}^{\sigma} n_{m'm}^{\sigma} \right) \right] \quad (1)$$

proposed in ref. 15 and implemented in VASP.¹⁴ The values of *U* and *J* are expressed through the Slater-Condon parameters *F^k* for the *d*- and *p*-shells according to:

$$\begin{aligned} U_{\text{C,N}} &= \alpha F_{\text{C,N}}^0; & J_{\text{C,N}} &= \frac{\alpha}{5} F_{\text{C,N}}^2 \\ U_{\text{V}} &= \alpha F_{\text{V}}^0; & J_{\text{V}} &= \alpha \frac{13}{112} F_{\text{V}}^2 \end{aligned} \quad (2)$$

The empirical values of the *F^k* parameters can be in principle extracted from the data on spectra of free atoms and ions of the corresponding elements (see Table 1). However, quantities thus obtained cannot be directly used in the LSDA+*U* context due to strong “screening” effects particularly important for *k* = 0. Meanwhile the approximation eq. (1) does not distinguish the difference in repulsions of electrons occupying different orbitals in the *d*-shell and treats these interactions in an average manner. For that reason the semiempirical values of *F^k*'s ref. 16 had been scaled uniformly by the factor *α* which had been adjusted to be equal to 0.4 resulting in the value of the *U* parameter of 5.344 eV for vanadium, which seems to be reasonable value, close to normally used in the LSDA+*U* context.

With these values the following numerical experiments have been undertaken. First, we performed the energy optimization for the original structure model of ref. 6 (Fig. 1). This model belongs to the *P4/mmm* space group (No. 123). Taking somewhat arbitrary parameters of the unit cell *a* = *b* = 6.413 Å, *c* = 8.736 Å (*V* = 359 Å³) corresponding to *d_{VN}* = 1.987 Å results in the number of unpaired electrons of 1.011 per unit cell (formula unit) which fairly corresponds to the picture when three unpaired electrons in the vanadium *d*-shell are partially compensated by two unpaired electrons

residing each in two TCNE radical anions. The corresponding density of states are shown in Figure 4 (left). The magnetic moments are predominantly concentrated in the vanadium *d*-shells (1.025). The rest comes from the organogenic atoms. However, the distribution of magnetization coming from the VASP modeling does not allow to single out any local momenta in the organic part. This can be possibly interpreted as a trend towards pairing the electrons in the TCNE radical anions on one hand and to pairing of electrons in the *d*-shells of vanadiums, which can be expected at that small unit cell volume. When the lattice parameters are optimized they relax towards the values *a* = *b* = 8.557 Å, *c* = 7.214 Å (*V* = 528 Å³); *d_{VN}* = 2.111 Å, which is fairly close to the values of ref. 6 *a* = *b* = 8.54 Å, *c* = 7.20 Å being in its turn in agreement with the experimental density.¹ At the optimized geometry the magnetization amounts 2.456 per formula unit. The magnetic moments are predominantly concentrated in the vanadium *d*-shells (1.959). The rest comes from the *p*-orbitals of the organogenic atoms. However, in this case either the distribution of magnetization coming from the VASP modeling does not allow to single out any local momenta in the organic part. The density of states for the relaxed structure of ref. 6 is represented in Figure 4 (right). It manifests some spin polarization of the bands in the range -1 ÷ -5 eV below the Fermi level. Meanwhile the uppermost filled bands in the range of 1 eV right below the Fermi level do not manifest almost any spin polarization. In analogy with the compressed structure one can expect that the trend towards pairing the electrons in the TCNE radical anions persists over the geometry relaxation, but on the other hand the tendency to pairing of electrons in the *d*-shells of vanadiums significantly reduces. These results indicate that the hypothetical structure of ref. 6 does not get an immediate support in the numerical experiment. Thus the situation requires more thorough investigation.

For this end we notice that setting the central C=C bonds of the TCNE units orthogonally to each other in the same plane in the “original” structure was (see Fig. 1) not the unique possibility. Alternatively one might consider a similar structure differing from that on Figure 1 by rotating one of the TCNE units entering the unit cell presented on Fig. 1 by 90° in its plane. The result of such a rotation is presented in Figure 5. In this structure the central C=C bonds of the TCNE units are as previously orthogonal, but now they lie in orthogonal planes as well so that the axes of these bonds do not intersect rather cross each other. For the reason which will be clear later we call this structure the “principal” structure. The principal structure with initial lattice parameters *a* = *b* = *c* = 7.14 Å (*V* = 364 Å³) yields the number of unpaired electrons to be 0.426 per formula unit. It can be characterized as a “poor metal.” The density of states in two spin channels is given in Figure 6 (left). One can see some (expectedly weak) spin polarization of the upper filled bands as well as a noticeable density of states at the Fermi level in both spin channels (in fact the Fermi level is close to the maxima of DOS of the corresponding bands). When the principal structure optimizes with the above parameters of the VASP calculation it relaxes to *a* = 8.181, *b* = 9.219, *c* = 7.484 Å (*V* = 564 Å³) with two nonequivalent *d_{VN}* = 2.18, 2.509 Å distances and the number of unpaired electrons 2.519 per unit cell (formula unit). The volume of the unit cell fairly corresponds to the observed density of the material.¹ Its electronic structure considerably differs from that of the “compressed” principal structure described above. It still can be characterized as that of a “poor metal.” The density of states

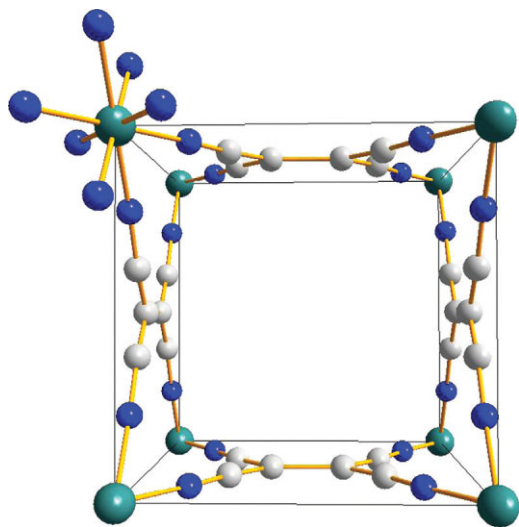


Figure 5. The “principal” structure of $V(TCNE)_2$ compound. Eight-coordination of vanadium ions is shown. The difference with the structure of the year 1993 is in the orientation of two TCNE units in two vertical faces of the shown unit cell. [Color figures can be viewed in the online issue, which is available at www.interscience.wiley.com.]

in two spin channels is given in Figure 6 (right). In variance with that of Figure 6 (left) the spin polarization is well developed below the Fermi level, where one can see a completely occupied subband with no obvious occupied counterpart of the opposite spin projection. It must be identified (on the basis of the DOS projection analysis) with the subband strongly hybridizing the p -shell of

TCNE units and the d -shells of vanadium (see later). Two shoulders above and below the main maximum apparently have filled counterparts of the opposite spin projection visible as well pronounced maxima of DOS. The highest completely filled band is strongly spin polarized as well: one of its subbands filled by electrons with spin projection coinciding with those in the presumed strongly hybridized p - d band is seen as an isolated peak right below the Fermi level. The counterpart of the former is the upper of two maxima slightly below it. This strongly spin-polarized band can be thought to be spanned by the acceptor states of one of the two TCNE molecules. This is manifested by the considerable asymmetry between them, which develops throughout the optimization procedure. As it has been mentioned in the optimized structure one can observe two V-N separations. The TCNE⁻ radical anion which is most strongly coordinated to vanadium (one with the shorter V-N interatomic separation) incidentally acquires a strong deformation of its own geometry: ethylenic C=C bond becomes 1.761 Å long, the single CC bond does not change too much (1.543 Å) as is the triple C≡N bond (1.209 Å). That strong elongation C=C bond may be a prerequisite for the spin polarization of the band stemming from it. At the same time the most weakly coordinated TCNE radical anion largely maintains its original structure: the ethylenic C=C bond is only 1.570 Å long, the triple C≡N bond is 1.205 Å long, and the main deformation is concentrated on the single CC bond which becomes 1.765 Å long. Turning back to the band structure of the relaxed principal structure of $V(TCNE)_2$ we mention only that there is a significant density of states at the Fermi level in both spin channels coming from the bands spanned by the TCNE anion radicals. This density at the Fermi level may serve as a prerequisite for consequent instabilities leading to more stable structures (see later).

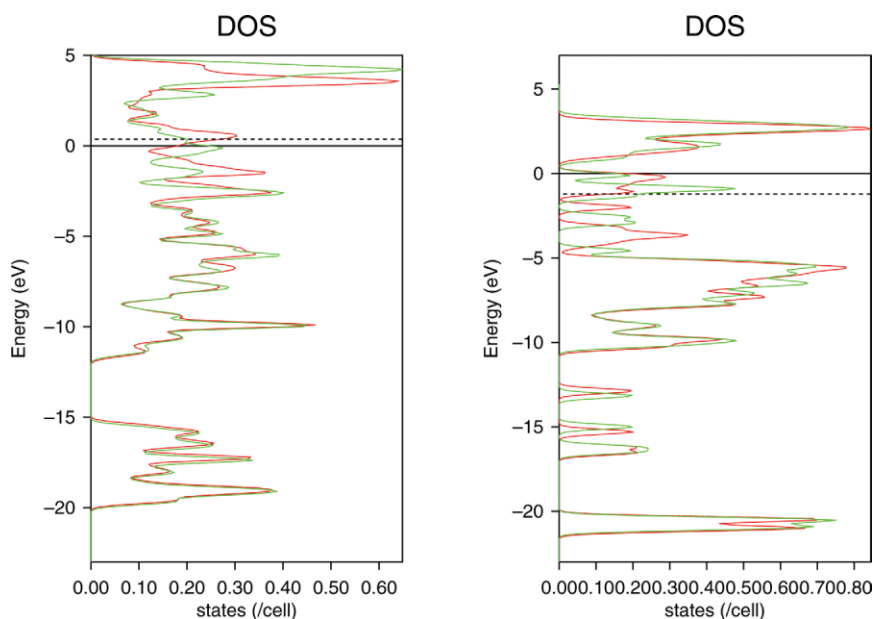


Figure 6. Density of states in two spin channels for the compressed (left) and relaxed (right) principal structures. [Color figures can be viewed in the online issue, which is available at www.interscience.wiley.com.]

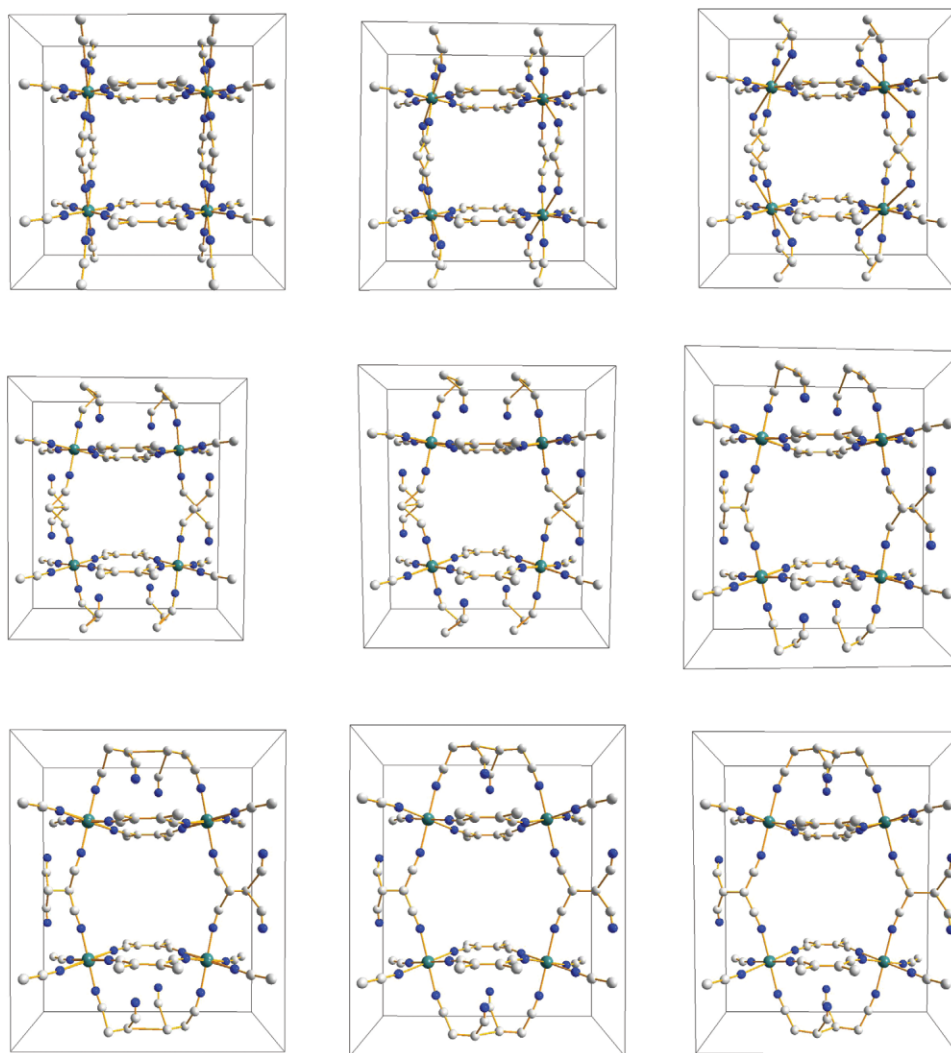


Figure 7. Schematic representation of the intermediate structures between the quadrupled “principal” (left upper corner) and the experimental (right lower corner) ones. [Color figures can be viewed in the online issue, which is available at www.interscience.wiley.com.]

The Fermi level in the relaxed “principal” structure lays close to the local DOS maximum. Thus it can be assumed that such a band might be sensitive to various symmetry breaking perturbations of the electronic and/or crystal structure. Indeed, authors of ref. 7 suggest that such a band as being half filled might undergo an antiferromagnetic metal-insulator transition. It is not completely true. The transitions accompanied by doubling of unit cell parameters in crystals with half-filled bands are not mandatory of whatever magnetic nature. These may be also structure transitions. What type of transition actually takes place is determined by the relative magnitude of the energy gain acquired throughout the transition of each respective type.

Bearing this in mind we notice that the principal structure can be relatively easily put in the connection with the experimental one. Indeed, as one can see the quadrupled unit cell $2a$, $2b$, c of the principal structure as presented on Figure 5 transforms to that of Figure 3 if one allows four TCNE units extended in the b direction and weakly

coordinating V atoms to rotate pairwise towards each other so that a C–C bond between respective ethylenic carbon atoms is formed yielding the $[\text{TCNE}]_2^{2-} = \text{C}_4(\text{CN})_8^{2-}$ dimers. Intermediate structures along this hypothetical reaction path are presented in Figure 7. For these structures we performed the VASP calculations of the respective electronic structures and energies. The calculations have been performed in two variants: first the principal structure with the equalized lattice parameters have been quadrupled and connected with the experimental structure by a straight line in the configuration space. These form the first sequence of studied structures. The second sequence is obtained by the same procedure but it starts at the quadrupled relaxed principal structure and ends in the experimental structure as well.

The results are presented in Table 2. As one can see after overcoming a relatively small energy barrier the quadrupled principal structure goes down in energy along the “reaction path” to some intermediate shallow minimum which corresponds to structures

Table 2. Energies and Magnetizations (Number of Spin-Up Electrons Minus That of Spin-Down per Unit Cell) for the Sequence of Structures of V(TCNE₂) Between the “Principal” and “Experimental” Ones.

No	Free energy (eV)	Magnetization	
0	-392.737780	1.908	11.115
1	-391.830207	2.446	11.194
2	-400.752426	3.417	3.801
3	-412.462565	5.028	5.454
4	-418.887744	5.457	
5	-420.108862	4.300	4.256
6	-419.543612	4.311	
7	-406.831963	4.052	6.160
8	-414.715571	5.582	6.522
9	-453.649124	8.019	8.366
10	-462.319179	8.016	

The energy column and the left column of magnetization represents the values referring to the points along the “reaction path” going from the compressed principal structure to the experimental structure; the right magnetization column refers to the points along the “reaction path” going from the relaxed principal structure to the experimental structure.

in the middle row of Figure 7. Next another barrier occurs after which the structure arrives to the experimental one of the iron compound (Fig. 3). The possibility that it can be considered as a prototype structure for the entire M(TCNE)₂ family will be studied elsewhere. The density of states for the spin-up and spin-down electrons for the last structure is presented in Figure 8 in such a way that the spin asymmetry of the DOS is better seen. In picture Figure 9 one can clearly see weakly spin polarized doubly occupied bands below -5 eV responsible for general bonding in the material. On the other hand, above -5 eV one can see several spin-polarized bands. Right above and below the Fermi level shown by the horizontal dashed line two symmetrical subbands appear one of which is completely filled whereas another is empty. The latter can be attributed to the (sub)bands spanned by LUMOs of the TCNE units. Below that, between two noticeably polarized bands one more subband of approximately triple intensity as compared to the above TCNE LUMO subband can be seen which is also completely filled but by electrons with the spin projection opposite to those filling the above TCNE LUMOs spanned subband. It can be attributed to the *d*-bands of vanadium ions. The magnetization in the last structure (that of the relaxed Fe(TCNE)₂) acquires the value of 8.016 unpaired electrons per unit cell which fairly corresponds to the picture of four vanadium atoms bearing the momenta of 3/2 pointing in one direction which are partially compensated by four 1/2 momenta located in four TCNE units and pointing in the opposite direction. On the stoichiometric grounds one can expect four more 1/2 momenta, which are, however, cancelled because of formation of two diamagnetic [TCNE]₂²⁻ = C₄(CN)₈²⁻ groups in each unit cell. Incidentally the Fe(TCNE)₂ structure substituted by V ions optimizes (as previously—first the unit cell parameters, then the positions of atoms in the relaxed unit cell) to a very close structure with the parameters *a* = 14.373, *b* = 17.472, *c* = 7.282, Å *β* = 90°, space group *C2/m* (group No 12). No remarkable difference between the local structures of the iron (experimental) and vanadium (hypothetical) compounds has been

found: *d*_{FeN} = 2.16 (axial), 2.19, 2.183 Å; *d*_{VN} = 2.16 (axial), 2.184, 2.19 Å.

One can see on the pictures of the density of states Figure 9 corresponding to the subsequent structures along the “reaction path” how the maxima of the spin DOS and other features at the Fermi level of the initial (quadrupled relaxed principal one) develop along the “reaction coordinate” going from it to the experimental one. The final electronic structure as compared to that initial one can be characterized as not one antiferromagnetically ordered, rather as a result of a structural transition driven by the C-C bond formation between TCNE⁻ radical-anions extended in the *b* direction. From the point of view of the band theory it is nothing but a Peierls-like rather than a Mott transition.

Magnetic properties of the intermediate structures are also of interest. The magnetization values corresponding to the structures depicted in Figure 7 are given in Table 2. It is of interest to compare the magnetizations obtained along the first sequence of structures (starting at the quadrupled compressed principal structure) and those obtained for the second sequence (starting at the quadrupled relaxed principal structure). As one could expect from the results of the calculation on the principal structure its relaxation results in a much stronger spin polarization. However, already small deformation towards the “experimental” structure along the corresponding “reaction path” (second sequence) switches the system to a state characterized by the values of magnetization close to those found along the first sequence of structures. It is remarkable that in the area of the intermediate shallow minimum (three structures in the middle row of Fig. 7) the magnetization values are close to those characteristic for the material obtained from V(C₆H₆)₂. At the end of both transition sequences (both referring to the “experimental” structure)

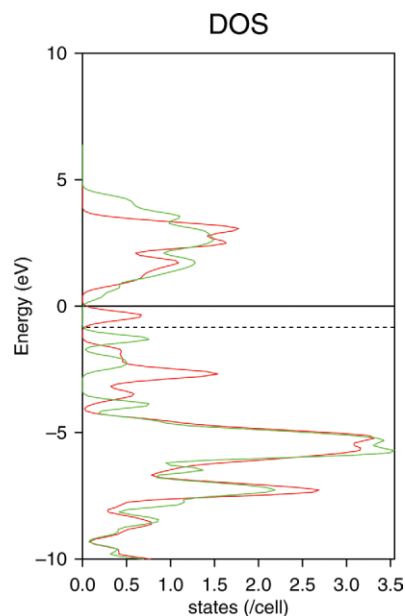


Figure 8. Spin-up and spin-down density of states of the V(TCNE)₂ compound obtained at the relaxed experimental geometry of the Fe(TCNE)₂ compound. [Color figures can be viewed in the online issue, which is available at www.interscience.wiley.com.]

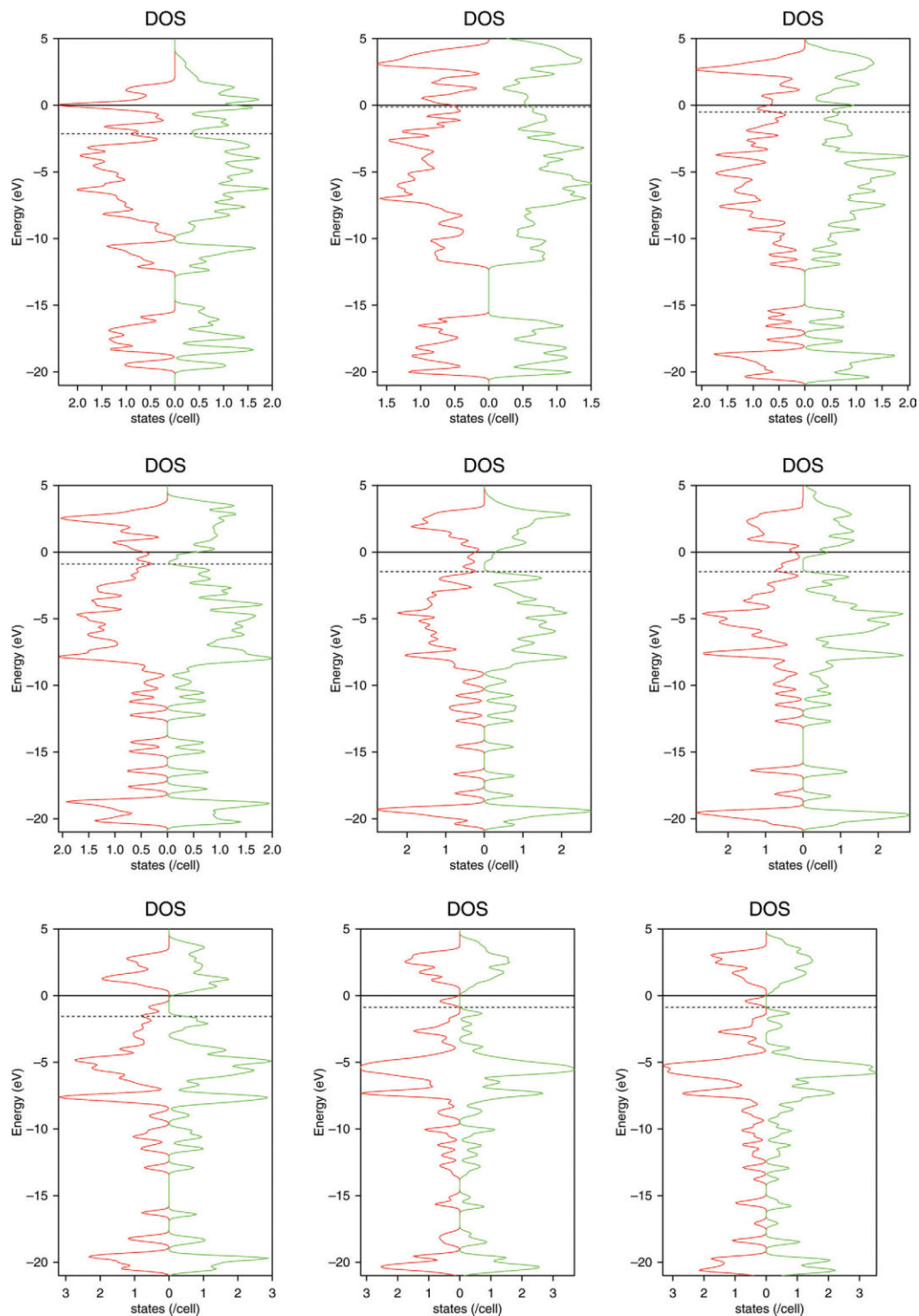


Figure 9. Densities of states in two spin channels for the intermediate structures between the quadrupled “principal” (left upper corner) and the experimental (right lower corner) ones (first sequence). [Color figures can be viewed in the online issue, which is available at www.interscience.wiley.com.]

the magnetization reaches the value of 8.016. That is something one could expect if a cell, containing one localized momentum 3/2 anti-ferromagnetically interacting with two localized momenta of 1/2, is quadrupled and then two of the four pairs of localized momenta 1/2 form a nonmagnetic state.

Namely the sign of the effective spin–spin interactions explains the reason why the total magnetic momentum per unit cell increases while going from the principal structure to the experimental one despite the simultaneous decrease of the number of magnetic centers in a unit cell.

The distribution of spin polarization in the direct space is also of importance. It is found that for all structures depicted in Figures 7 the magnetic moments residing on vanadium ions are almost constant and range from 2.615 for the first structure to 2.582 for the last one in the second sequence. The observed (in our numerical experiment) significant variation of magnetic moment along the “reaction path” must be almost entirely attributed to variation of the magnetic moments residing in the “organic” part of the organometallic magnet. This is precisely what one should expect within the general picture including formation of $[\text{TCNE}]_2^{2-}$ dimers.

Model Hamiltonian for V-TCNE System and Related Band Structure

The results of numerical modeling obtained in the previous Section call for some qualitative discussion. It can be given in terms of an effective model Hamiltonian representing the electronic structure of the $\text{V}(\text{TCNE})_2$ magnet (in its “experimental” structure), similar to that proposed yet in ref. 6. The general methodology of constructing such Hamiltonians is based on a heuristic search of the most important one-electron states contributing to the energy bands in the vicinity of the Fermi level. The physical reason for the search for such a construct is rather obvious: namely the electron transitions between the bands in the close vicinity of the Fermi level are the low-energy excitations of the solid responsible for its observable properties controlled by its response to the low-energy perturbations. From certain point of view one may think that heavy numerical modeling tools (like VASP) merely provide parameters for such effective states and for the Hamiltonians describing their interactions. The original model Hamiltonian for the $\text{V}(\text{TCNE})_2$ magnet proposed in ref. 6 used such a restricted set of one-electron states as described in the Introduction: namely the d -states of vanadium ions and the $b_{3g}(\pi^*)$ LUMOs of the TCNE (singly occupied in the radical anion). The electronic structure calculations by VASP for the original structure fairly manifest the characteristic features of the required effective model (the p - and d -states). The effective Hamiltonian for the “principal” model constructed on the same set of one-electron states differs from the “original” model by phase factors (see later). The VASP calculations of the electronic structure of the “principal” arrangement of the building blocks of the organometallic ferromagnet also manifests the characteristic one-electron states required for constructing the effective model.

On the other hand the “experimental” structure differs quite strongly from the “principal” structure. The main difference is the formation of diamagnetic $\text{C}_4(\text{CN})_8^{2-}$ units which leads to effective isolation of the $\text{V}(\text{TCNE})$ sheets. Thus of the primary importance must be the Hamiltonian for the separate ruffled V-TCNE plane. One can employ for constructing the Hamiltonian for this plane the

unit cell of the principal model dropping from it the TCNE unit extended to the b direction (and finally engaged in formation of the $[\text{TCNE}]_2^{2-} = \text{C}_4(\text{CN})_8^{2-}$ dimers) and extending the rest in the a and c directions (neglecting the ruffling). In each such a sheet each metal ion is surrounded (coordinated) by four TNCE units which are in their turn coordinated to (surrounded by) four metal atoms.

On the vanadium sites it suffices to consider only the d -shells of the metal ions. The overlap of the d -shell with the σ -orbitals of the TCNE’s (including those implied in the model) ensures the standard two-over-three splitting of the d -shell characteristic for the octahedral environment. In case of vanadium it means that the three unpaired electrons in the d -shell occupy respectively three orbitals in the t_{2g} -manifold. The d_{xy} -, d_{xz} -, and d_{yz} -orbitals can be characterized by the normal to the plane in which each of the orbitals lays – ζ , η , and ξ – and subsequently used in the notation.

The model Hamiltonian for the $\text{V}(\text{TCNE})_2$ magnet, formulating the above ideas, has the general form:

$$H = \sum_{\mathbf{r}} (H_d(\mathbf{r}) + H_a(\mathbf{r}) + H_{da}(\mathbf{r}) + H_{dd}(\mathbf{r})) \quad (3)$$

Operator $H_a(\mathbf{r})$ describes electrons in the acceptor orbital of the TCNE^- radical-anion in the \mathbf{r} -th unit cell:

$$H_a(\mathbf{r}) = (-\alpha_a \hat{n}_{a\mathbf{r}} + U_{aa} \hat{n}_{\mathbf{r}\downarrow} \hat{n}_{\mathbf{r}\uparrow}) \quad (4)$$

$$\hat{n}_{a\mathbf{r}\sigma} = a_{\mathbf{r}\sigma}^+ a_{\mathbf{r}\sigma}; \hat{n}_{a\mathbf{r}} = \sum_{\sigma} \hat{n}_{a\mathbf{r}\sigma}$$

Quantities $a_{\mathbf{r}\sigma}^+$ ($a_{\mathbf{r}\sigma}$) are the operators creating (annihilating) an electron with spin projection σ on the acceptor orbitals of the TCNE molecules in the \mathbf{r} -th unit cell. In eq. (4) the first term is the energy of attraction of an electron to the core of TCNE – the orbital energy of the $b_{3g}(\pi^*)$ LUMO shifted by the electrostatic field induced by the entire crystal environment. The second term is the Hubbard one, effectively describing the Coulomb repulsion of electrons with opposite spin projections eventually occupying the same acceptor orbital.

The operator $H_d(\mathbf{r})$ describes electrons in the d -shell of the vanadium ion in the \mathbf{r} -th unit cell:

$$H_d(\mathbf{r}) = [-\alpha_d (\hat{n}_{\zeta\mathbf{r}} + \hat{n}_{\eta\mathbf{r}} + \hat{n}_{\xi\mathbf{r}}) + (U_{dd} + 2J_{dd}) (\hat{n}_{\zeta\mathbf{r}\downarrow} \hat{n}_{\zeta\mathbf{r}\uparrow} + \hat{n}_{\eta\mathbf{r}\downarrow} \hat{n}_{\eta\mathbf{r}\uparrow} + \hat{n}_{\xi\mathbf{r}\downarrow} \hat{n}_{\xi\mathbf{r}\uparrow})] + \frac{(U_{dd} + J_{dd}/2)}{2} \sum_{\sigma, \sigma'} (\hat{n}_{\zeta\mathbf{r}\sigma} \hat{n}_{\xi\mathbf{r}\sigma'} + \hat{n}_{\zeta\mathbf{r}\sigma} \hat{n}_{\eta\mathbf{r}\sigma'} + \hat{n}_{\xi\mathbf{r}\sigma} \hat{n}_{\eta\mathbf{r}\sigma'}) - 4J_{dd} (\hat{S}_{\zeta\mathbf{r}} \hat{S}_{\xi\mathbf{r}} + \hat{S}_{\zeta\mathbf{r}} \hat{S}_{\eta\mathbf{r}} + \hat{S}_{\xi\mathbf{r}} \hat{S}_{\eta\mathbf{r}}) \quad (5)$$

$$\hat{n}_{\gamma\mathbf{r}\sigma} = \gamma_{\mathbf{r}\sigma}^+ \gamma_{\mathbf{r}\sigma}; \hat{n}_{\gamma\mathbf{r}} = \sum_{\sigma} \hat{n}_{\gamma\mathbf{r}\sigma}; \gamma = \xi, \eta, \zeta.$$

In eq. (5) the quantities $\zeta_{\mathbf{r}\sigma}^+$ ($\zeta_{\mathbf{r}\sigma}$), $\xi_{\mathbf{r}\sigma}^+$ ($\xi_{\mathbf{r}\sigma}$), and $\eta_{\mathbf{r}\sigma}^+$ ($\eta_{\mathbf{r}\sigma}$) are the operators creating (annihilating) an electron with spin projection σ on the d_{xy} , d_{yz} , and d_{xz} orbitals, respectively, of the vanadium ion in the \mathbf{r} -th unit cell. The first term in the above operator describes the attraction of electrons in the d -orbitals to the atomic cores (shifted by the electrostatic field of the rest of the crystal). Our experience shows that the crystal field splitting between the d -states in the ligand

environment with that small asymmetry as described in the above Section must be negligible as compared to the intraatomic energies.

The spin operators and spin-operator product terms are defined by the well-known relations:

$$\hat{S}_\gamma \hat{S}_{\gamma'} = 1/2(\hat{S}_\gamma^+ \hat{S}_{\gamma'}^- + S_\gamma^+ S_{\gamma'}^-) + \hat{S}_\gamma^z \hat{S}_{\gamma'}^z$$

$$S_\gamma^+ = \gamma_\uparrow^+ \gamma_\downarrow, \hat{S}_\gamma^- = \gamma_\downarrow^+ \gamma_\uparrow, \hat{S}_\gamma^z = 1/2(\hat{n}_{\gamma\uparrow} - \hat{n}_{\gamma\downarrow}).$$

Operator $H_{da}(\mathbf{r})$ describes electron hopping interaction between the d -states of vanadium ions and the acceptor states. The d_{xy} -state represented by the $\zeta_{\mathbf{r}\sigma}^+$ ($\zeta_{\mathbf{r}\sigma}$) operators being of the (approximate) σ -symmetry with respect to the ac plane (ruffled V-TCNE plane) has no overlap with the LUMO's of TCNE's which are of the π -symmetry with respect to the same plane. Two others (d_{xz} - and d_{yz} -states represented respectively by the $\eta_{\mathbf{r}\sigma}^+$ ($\eta_{\mathbf{r}\sigma}$) and $\xi_{\mathbf{r}\sigma}^+$ ($\xi_{\mathbf{r}\sigma}$) operators) overlap with the LUMOs of two neighbor TCNE units each. The phase relations between the orbitals involved in the model lead to the following distribution of signs at the one-electron hopping integrals between the orbitals. This produces the contribution to the Hamiltonian of the form:

$$H_{da}(\mathbf{r}) = -t_{da} \sum_{\sigma} [\xi_{\mathbf{r}\sigma}^+ (a_{\mathbf{r}\sigma} + a_{\mathbf{r}+\mathbf{a}+\sigma}) - \eta_{\mathbf{r}\sigma}^+ (a_{\mathbf{r}+\mathbf{a}\sigma} + a_{\mathbf{r}+\mathbf{c}\sigma})] + h.c. \quad (6)$$

where the parameter $t_{da} > 0$ describes the magnitude of the hopping between the acceptor state and the nearest neighbor d -state.

The sum of the contributions to the effective Hamiltonian in fact form that for isolated V-TCNE layers. Meanwhile, one should assume that certain indirect delocalization of the d -states in the b -direction is possible through the mediation of the $[\text{TCNE}]_2^-$ units. On the symmetry grounds one may expect the following additional term in the Hamiltonian coupling different V-TCNE layers:

$$H_{dd}(\mathbf{r}) = -t_{dd} \sum_{\gamma,\sigma} \gamma_{\mathbf{r}\sigma}^+ \gamma_{\mathbf{r}+\mathbf{b}\sigma} + h.c.; \gamma = \xi, \eta, \zeta. \quad (7)$$

One can also expect certain effective hopping within each V-TCNE layer also mediated by the $[\text{TCNE}]_2^-$ units extended in the a -direction. But this latter can be expected to be significantly weaker than the direct V-TCNE hopping ($t_{da} \gg t_{dd}$) and thus can be neglected. By contrast the interlayer hopping of the same magnitude and occurring due to the same mechanism is the only source of tentative delocalization in the b -direction and thus has to be retained.

Band Structure as Derived from the Model Hamiltonian

The suggested Hamiltonian defined by eqs. (3)–(7) suffices for analysis of the basic results of the above numerical experiments performed with use of the VASP package.¹⁴ The latter implements in a way the general self consistent field (SCF) approximation to the “exact” ground state of the Hamiltonian for the crystal. The SCF

approximation reduces to factorizing the terms of electron–electron interaction in the Hamiltonian according to the rule:

$$c_1^+ c_2 c_3^+ c_4 \rightarrow (c_1^+ c_2) c_3^+ c_4 - (c_1^+ c_4) c_3^+ c_2 \quad (8)$$

by this yielding the Fockian of the system. The averages (\dots) are to be calculated over the single determinant approximate ground state of the crystal, which is yet to be found. The general form of the averages involved in the expression eq. (8) can be chosen semiempirically to satisfy a priori (largely symmetry-based) conditions characterizing the ground state of interest. For instance, the averages of the form $\langle c_\sigma^+ c_{-\sigma} \rangle$ are set to be zero. This is equivalent to requiring that the ground state is an eigenstate of the spin projection operator. Hence all the averages of the form $\langle \hat{S}^+ \rangle$ or $\langle \hat{S}^- \rangle$ are zero as well. We also assume the averages to be the same for all unit cells (*i.e.* independent on \mathbf{r}) so that no superstructure develops in the V-TCNE layers (see although below). The quantities $\langle \hat{n}_{\gamma\mathbf{r}\sigma} \rangle$ and $\langle \hat{S}_{\gamma\mathbf{r}}^z \rangle$ are then the \mathbf{r} -independent averages of the operators $\hat{n}_{\gamma\mathbf{r}\sigma}$ and $\hat{S}_{\gamma\mathbf{r}}^z$ over the ground state.

To find the ground state for the crystal we apply the spin unrestricted Hartree-Fock (UHF) version of the SCF approximation, which produces the dispersion laws for the electron bands of the crystal and other quantities relevant for the solution.

The parameter

$$\frac{t_{da}}{\Delta\alpha_\sigma} \ll 1 \quad (9)$$

(see later) is small since its denominator is controlled by the large energy separation between the electron affinities of the neutral TCNE unit α_a and that of the $3d$ -orbitals of the vanadium dication coordinated by six CN groups coming from four TCNE's and two $\text{C}_4(\text{CN})_8^{2-}$'s. This results in the following picture of narrow bands (the effective width is scaled down by the above small parameter):

$$\begin{cases} -\alpha_{a\sigma} + \frac{t_{da}^2}{\Delta\alpha_\sigma} (Q_{\mathbf{k}\xi}^* Q_{\mathbf{k}\xi} + Q_{\mathbf{k}\eta}^* Q_{\mathbf{k}\eta}); & \text{for the “+” sign} \\ -\alpha_{\mathbf{k}d\sigma} - \frac{t_{da}^2}{\Delta\alpha_\sigma} (Q_{\mathbf{k}\xi}^* Q_{\mathbf{k}\xi} + Q_{\mathbf{k}\eta}^* Q_{\mathbf{k}\eta}); & \text{for the “-” sign} \\ -\alpha_{\mathbf{k}d\sigma}; & \text{doubly degenerate} \end{cases}$$

$$\Delta\alpha_\sigma \approx |\alpha_{a\sigma} - \alpha_{d\sigma}|, \quad (10)$$

where we neglect the \mathbf{k} -dependence in the denominator and keep it in the form-factors $Q_{\mathbf{k}\xi}$ and $Q_{\mathbf{k}\eta}$ defined (together with other quantities) in the Appendix.

The above (nonvanishing) effective bandwidths must be compared with the on-site electron–electron interaction parameters U_{aa} and U_{dd} which play the rôles of the Stoner factors for the respective bands. Since

$$U_{aa}, U_{dd} \gg \frac{t_{da}^2}{\Delta\alpha_\sigma}; \quad t_{dd}$$

one may expect that in each case only the subbands corresponding to only one of two possible spin projections is filled in the lower band of the two of eq. (10). This results in the ferromagnetic order

for electrons in each band. It is obviously so for two d -bands of “ t_{dd} ” width and for the band described by the second row in eq. (10)—one marked as ‘for the “-” sign.’ As for the band spanned by the acceptor states (LUMO’s of the TCNE units—the first row in eq. (10)) it can become populated if its lower edge occurs at an energy lower than that of either of so far empty subbands spanned by the d -orbitals. This is assured by the relative magnitude of the energy gap between the empty flat d -subbands and the acceptor subbands. It is controlled by the relation between the parameters $\Delta\alpha_\sigma$ and U_{dd} . On the basis of analysis of the results of our numerical experiment it can be safely concluded that the intersubband d - d gap U_{dd} is larger than the gap $\Delta\alpha_\sigma$ so that the acceptor spanned subband is populated. As in the case of the d -bands the intramolecular repulsion parameter U_{aa} assures that only one of two acceptor subbands is populated by electrons.

Now let us address the interaction between the completely spin-polarized (ferromagnetically ordered) bands spanned respectively by the TCNE LUMOs and the vanadium d -shells. As in the model⁶ the resonance (one-electron hopping) between the acceptor states and the d -states dominates. These interactions are described by the $H_{da}(\mathbf{r})$ operators. Because of the structure of the spin-polarized SCF theory the corresponding hopping parameter t_{da} appears in the result only through the corresponding effective band widths. Correspondingly the relative orientation of the electronic spins in the occupied d - and acceptor subbands is determined by the relative position of the acceptor subband corresponding to the spin projection $\tau = \pm\sigma$ on the energy scale, provided the d -subbands corresponding to the spin projection σ are occupied. This is determined by the requirement of minimizing the energy per formula unit also given in the Appendix which yields that namely the acceptor spanned subband with $\tau = -\sigma$ is lower in energy and thus is populated.

The DOS coming from the model band Hamiltonian is depicted in Figure 10. It fairly reproduces the most important features of numerical (VASP) DOS as shown in Figure 9.

Finally we can address the relation between the Hamiltonian proposed in the present paper and that of ref. 6. One can notice that the key difference between the two is the presence of one more acceptor band in the model of ref. 6 coming from the second acceptor unit in the minimal unit cell required by stereochemistry. The following events can be described as follows. First of all we notice that despite the fact that the unit cell of the experimental structure is quadrupled as compared to that of the principal one it is enough to consider the unit cell doubled in the a -direction: $2a, b, c$. Then according to the band folding scheme (see ref. 19) the number of bands doubles. The electron count is such that the acceptor bands which are almost flat (small dispersion) are half filled. This is a prerequisite for these bands to be sensitive to whatever perturbation mixing the states with the same value of \mathbf{k} relative to the doubled unit cell. As one can check introducing a modulation of the one-electron hopping integrals between the acceptor orbitals localized on the TCNE units extended in the b -direction (in the principal structure they are assumed to be zero) can serve as a required perturbation. It splits the folded acceptor band into two bands such that one of them sinks among other occupied bands. In plain words this can be interpreted as pairing of electrons located on the TCNE⁻ units which upon pairing – forming the C–C bonds cannot be used to compensate the momenta located on the V ions.

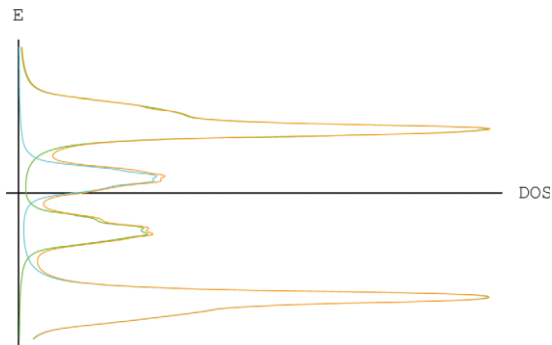


Figure 10. Model density of electronic states of V(TCNE)₂ (in red) in two spin channels (respectively green and blue) (principal structure) as derived from the model Hamiltonian eq. (3). The occupied subbands spanned by the d -states and acceptor states respectively belong to the channels with opposite spin projections. [Color figures can be viewed in the online issue, which is available at www.interscience.wiley.com.]

The spin polarization of the solution is assured by the fact that if the α -subbands of three predominantly d -bands are completely filled the β -subband of the predominantly acceptor bands is lower in energy and for that reason is populated first. The total contribution of electron hopping between the acceptor orbitals and the d -orbitals is obtained by the integration of the contribution

$$-\frac{t_{da}^2}{\Delta\alpha_\sigma} (Q_{\mathbf{k}\xi}^* Q_{\mathbf{k}\xi} + Q_{\mathbf{k}\eta}^* Q_{\mathbf{k}\eta}), \quad (11)$$

which is the energy coming from the antiferromagnetic coupling between electrons occupying respectively the \mathbf{k} -th Bloch sum of the acceptor states with the respective combination of the \mathbf{k} -th Bloch sums of the d -state, over the Brillouin zone and summing over the spin projections σ .

Discussion

In the present article we performed numerical studies of the structural models of V-TCNE room temperature organometallic “ferromagnet” and analyzed the result in terms of the effective Hamiltonian for a selection of interacting atomic/molecular states and related band picture. It turns out that the results of numerical study can be fairly interpreted in terms of the proposed model.

It makes thus sense to apply the proposed models to analysis of a wider collection of experimental data available on this fascinating objects. First of all we notice that the spin polarization per unit cell (number of electrons with spin up minus that with spin down) which can be related with observed magnetization per formula of the compound at hand. We see that the calculation performed for the experimental structure 1 (spin polarization *ca.* 8 spins-1/2 per unit cell corresponding to two net unpaired electrons per V atom) is in a fair agreement with the magnetization measured in the V-TCNE compound prepared from V(CO)₆. On the other hand the original material prepared from V(C₆H₆)₂ manifests a weaker saturation magnetization, namely corresponding to *ca.* one unpaired electron per V atom. This allows to think about certain differences in the

structures of two materials, described below, as dependent on the way of their fabrication. Nevertheless both experimentally observed values (about 10×10^3 emuOe mol⁻¹ and 6×10^3 emu Oe mol⁻¹, respectively) both deviate from the theoretical values of 11.2 and 5.6 giving the magnetization produced by the integer number of net spin-polarized electrons in an assumption of the Landé being equal to 2. Remarkable is that in a more magnetized material the experimental magnetization seems to be smaller than the theoretical value whereas in a less magnetized material it is larger than the theoretical one.

Turning to analysis of the obtained band structure in the vicinity of the Fermi level we notice that the main contribution to relative shifts of the subbands corresponding to different spin-projections comes from the on-site electron–electron repulsion integrals U_{dd} and U_{aa} . That means that the empty d -subbands are shifted upwards by U_{dd} as compared to the filled ones, whereas the empty acceptor subband is shifted upwards by U_{aa} relative to the occupied one. The pair of the acceptor subbands is well seen in the DOS picture Figure 9 which allows us to estimate the latter value to be 0.9 eV. This is in fair agreement with the estimate of ref. 7 based on magnetoresistivity data. One has to notice only that the formula used in ref. 7 to estimate the concentration of carriers is corrected to take into account the fact that the holes in the occupied subband arising when the electrons are excited to the conduction subband serve as carriers as well. This results in the factor of 1/2 (see ref. 20) relating the one-electron gap U_{aa} with the thermal activation energy entering the exponential function for the carriers' concentration.

When trying to extend their model¹⁰ to analysis of the V-TCNE compounds these authors argue that the vanadium compound must have somewhat different structure since the saturation magnetization in it is lower and approximately corresponds to two spins 1/2 compensating (interacting antiferromagnetically with) one spin 3/2 per formula unit. From this observation the authors of¹⁰ conclude that the interlayer interactions must be mediated by μ_4 -TCNE radical-anions, as it has been suggested yet in.⁶ From the point of view of the spin-Hamiltonian model ref. 6 the existence of the effective spins $S_V = 3/2$ on the vanadium sites is assured by the strong intrashell interaction J_{dd} having order of $10^3/10^4$ K. In this respect our results agree with the suggestions of ref. 10. On the other hand our numerical experiment shows that for the relaxed experimental structure the calculated magnetization fairly corresponds to experimental value obtained on V-TCNE material derived from V(CO)₆. Incidentally, the magnetization values obtained numerically at intermediate structures on the “reaction path” depicted in Figure 7 allows us to assume that some similar structures may present in the V-TCNE material derived from V(C₆H₆)₂.

Conclusion

In the present article we performed extensive numerical studies on thinkable structures of room-temperature organometallic magnet V(TCNE)₂ and obtained corresponding densities of one-electron states, magnetizations, and other characteristics of the considered structures. Model band Hamiltonian is developed for analysis and interpretation of numerical results and experimental data. Careful analysis of magnetic data in terms of the models is performed. A remarkable correspondence between experimental (structural and

magnetic) data on V(TCNE)_x × *y* solvent and numerical model is already observed: magnetization corresponding to two unpaired electrons per formula unit in remarkable agreement with experiment on V-TCNE material derived from V(CO)₆ is obtained numerically for V(TCNE)₂ taken in the relaxed experimental Fe(TCNE)₂ structure; magnetization approximately corresponding to one unpaired electrons per formula unit in fair agreement with experiment on V-TCNE material derived from V(C₆H₆)₂ is obtained numerically for intermediate structures between that of Fe(TCNE)₂ and the structure proposed in ref. 6.

Acknowledgments

ALT is thankful to Drs B. Eck, J. von Appen, and A. Houben and to Mr. M. Gilleßen for their help in mastering the solid state electronic structure software at the IAC of the RWTH. The authors are thankful to Prof. J.S. Miller for his valuable comments on reported experimental data.

Appendix: Details of Analytical Treatment of Band Model of the “Experimental” Structure

Applying the spin-unrestricted Hartree–Fock approximation to the model Hamiltonian eq. (3) leads to the Fockian composed of two individual components for the spatial states occupied by electrons of each spin projection. The Fockian for a given spin-projection depends on the population of the states with the opposite spin projection. In the solid-state (translationally invariant) context these Fockian blocks significantly simplify by going to the Fourier transforms (the Bloch sums) of the Fermi operators $a_{\mathbf{k}\sigma}$ and $\gamma_{\mathbf{k}\sigma}$, $\gamma = \zeta, \eta, \xi$:

$$\begin{aligned} a_{\mathbf{k}\sigma} &= (N)^{-1/2} \sum_{\mathbf{r}} \exp(-i\mathbf{k}\mathbf{r}) a_{\mathbf{r}\sigma}; \\ \gamma_{\mathbf{k}\sigma} &= (N)^{-1/2} \sum_{\mathbf{r}} \exp(-i\mathbf{k}\mathbf{r}) \gamma_{\mathbf{r}\sigma}. \end{aligned} \quad (\text{A1})$$

In this new basis the Fockian component for the spin projection σ becomes a direct sum over the wave vector \mathbf{k} of the 4×4 matrix blocks:

$$\begin{aligned} F_{\text{band}}^{\sigma} &= \bigoplus_{\mathbf{k}} F^{\sigma}(\mathbf{k}) \\ F^{\sigma}(\mathbf{k}) &= \begin{pmatrix} -\alpha_{\zeta\mathbf{k}\sigma} & 0 & 0 & 0 \\ 0 & -\alpha_{\xi\mathbf{k}\sigma} & 0 & -t_{da}Q_{\mathbf{k}\xi} \\ 0 & 0 & -\alpha_{\eta\mathbf{k}\sigma} & -t_{da}Q_{\mathbf{k}\eta} \\ 0 & -t_{da}Q_{\mathbf{k}\xi}^* & -t_{da}Q_{\mathbf{k}\eta}^* & -\alpha_{a\sigma} \end{pmatrix} \\ \alpha_{a\sigma} &= \alpha_a - U_{aa}n_{a-\sigma} \\ \alpha_{\gamma\mathbf{k}\sigma} &= \alpha_d - 2t_{dd} \cos \mathbf{k}b - (U_{dd} + 2J_{dd})n_{\gamma-\sigma} \\ &\quad - (U_{dd} + J_{dd}/2) \sum_{\tau, \kappa \neq \gamma} n_{\kappa\tau} + 4J_{dd}\sigma \sum_{\kappa \neq \gamma} S_{\kappa}^z \end{aligned} \quad (\text{A2})$$

where \oplus stands for the direct sum of the above matrices; quantities $n_{a\sigma}, n_{\gamma\sigma}, S_{\gamma}^z$ – for the translationally invariant averages of the respective operators over the ground state of the system. On the symmetry grounds one can also assume that the quantities $n_{\gamma\sigma}$ and S_{γ}^z are both γ -independent ($n_{\gamma\sigma} \approx 0, 1; S_{\gamma}^z \approx \sigma$, provided $n_{\gamma\sigma} \approx 1$) so that for all γ $\alpha_{\gamma k\sigma} = \alpha_{dk\sigma}$ (see later).

First three rows of each 4×4 matrix block correspond to the Bloch sums of the atomic ζ -, η -, and ξ -states, respectively, and the fourth row corresponds to the Bloch sum of the acceptor states. The Fockian dependence on \mathbf{k} involves the form-factors:

$$Q_{k\xi} = 1 + \exp(-i\mathbf{k}_a - i\mathbf{k}_c) \quad (\text{A3})$$

$$Q_{k\eta} = -[\exp(-i\mathbf{k}_a) + \exp(-i\mathbf{k}_c)] \quad (\text{A4})$$

The eigenvalues of the above 4×4 matrices can be easily written as functions of \mathbf{k} by noting first, that the band spanned by the ζ -states is not involved in any interaction and thus its width comes only from the interlayer hopping, and then by going to the linear combinations:

$$\begin{aligned} S_{k\eta}\xi_{k\sigma} + S_{k\xi}\eta_{k\sigma} \\ S_{k\xi}\xi_{k\sigma} - S_{k\eta}\eta_{k\sigma} \end{aligned} \quad (\text{A5})$$

of the η - and ξ -states, where the phase factors $S_{k\gamma}$ the are given by:

$$S_{k\xi} = Q_{k\xi} (Q_{k\xi}^* Q_{k\xi} + Q_{k\eta}^* Q_{k\eta})^{-\frac{1}{2}} \quad (\text{A6})$$

$$S_{k\eta} = Q_{k\eta} (Q_{k\xi}^* Q_{k\xi} + Q_{k\eta}^* Q_{k\eta})^{-\frac{1}{2}} \quad (\text{A7})$$

This results in four pairs of narrow subbands spanned by the states of respective spin projection. Two pairs of them have (in the present model) the bandwidth of $2t_{dd}$ (the ζ -band and that given by the second linear combination of the η - and ξ -Bloch sums in eq. (A6). They are incidentally degenerate both having the energy $\alpha_{dk\sigma}$ which turns out to be

$$\begin{aligned} \alpha_{dk\sigma} = \alpha_d + 2t_{dd} \cos \mathbf{k}_b - 2(U_{dd} + J_{dd}/2) \\ + \begin{cases} -(U_{dd} + 4J_{dd}) & \text{for empty subband} \\ 2J_{dd}, & \text{for filled subband} \end{cases} \quad (\text{A8}) \end{aligned}$$

Two other subbands have the form:

$$-\frac{\alpha_{dk\sigma} + \alpha_{a\sigma}}{2} \pm \sqrt{\frac{(\alpha_{dk\sigma} - \alpha_{a\sigma})^2}{4} + t_{da}^2 (Q_{k\xi}^* Q_{k\xi} + Q_{k\eta}^* Q_{k\eta})}$$

Keeping in mind the symmetry-conditioned restrictions on the form of the averages imposed above, we obtain, after some algebra, the electronic energy of the crystal per unit cell in the UHF

approximation:

$$\begin{aligned} E = -\alpha_a n_{a\sigma} + U_{aa} n_{a\uparrow} n_{a\downarrow} + (U_{dd} + 2J_{dd}) \sum_{\gamma} n_{\gamma\uparrow} n_{\gamma\downarrow} \\ + \frac{(U_{dd} + J_{dd}/2)}{2} \sum_{\sigma, \tau} (n_{\zeta\sigma} n_{\xi\tau} + n_{\zeta\sigma} n_{\eta\tau} + n_{\xi\sigma} n_{\eta\tau}) \\ - 4J_{dd} (S_{\zeta}^z S_{\xi}^z + S_{\zeta}^z S_{\eta}^z + S_{\xi}^z S_{\eta}^z) - t_{da} \sum_{\sigma} P_{\sigma}^{da} - t_{dd} \sum_{\sigma} P_{\sigma}^{dd} \end{aligned}$$

where the averages of the electron hopping operators are defined by

$$\begin{aligned} P_{\sigma}^{da} &= (\langle \xi_{r\sigma}^+ a_{r\sigma}^+ \rangle + \langle \xi_{r\sigma}^+ a_{r+a+c\sigma} \rangle) - (\langle \eta_{r\sigma}^+ a_{r+a\sigma} \rangle + \langle \eta_{r\sigma}^+ \zeta_{r+c\sigma} \rangle) \\ P_{\sigma}^{dd} &= \sum_{\gamma} \langle \gamma_{r\sigma}^+ \gamma_{r+b\sigma} \rangle \end{aligned}$$

As one can check the P_{σ}^{dd} average vanishes due to fact that the corresponding subbands are either completely occupied or completely empty. The term containing the sum of P_{σ}^{da} in fact gives the energy of interaction of occupied d - and acceptor subbands, which can be calculated immediately. Indeed, as we mentioned previously, the only interaction between the d - and acceptor states is the sum of $H_{da}(\mathbf{r})$ operators. In the basis of the Bloch sums eqs. (A1), (A6) this operator yields only one nonvanishing matrix element

$$-t_{da} (Q_{k\xi}^* Q_{k\xi} + Q_{k\eta}^* Q_{k\eta})^{\frac{1}{2}} \quad (\text{A9})$$

coupling the \mathbf{k} -th Bloch sum of the acceptor states with the first of the two \mathbf{k} -th Bloch sums of the d -states eq. (A6). The energy gain is only possible if the occupancies of the interacting subbands are opposite: so if the α - (spin up) subband of the d -band is filled the corresponding subband of the acceptor band must be empty and vice versa – otherwise no hopping between the occupied states is possible.

References

- Manriquez, J. M.; Yee, G. T.; McLean, S. R.; Epstein, A. J.; Miller, J. S. Science 1991, 252, 1415.
- Vickers, E. B.; Selby, T. D.; Miller, J. S. J Am Chem Soc 2004, 126, 3716.
- Vickers, E. B.; Selby, T. D.; Thorum, M. S.; Taliaferro, M. L.; Miller, J. S. Inorg Chem 2004, 43, 6414.
- Taliaferro, M. L.; Thorum, M. S.; Miller, J. S. Angew Chem Int Ed 2006, 45, 5326.
- Pokhodnya, K. I.; Vickers, E. B.; Bonner, M.; Epstein, A. J.; Miller, J. S. Chem Mater 2004, 16, 3218.
- Tchougréeff, A. L.; Hoffmann, R. J Phys Chem 1993, 97, 350.
- Prigodin, V. N.; Raju, N. P.; Pokhodnya, K. I.; Miller, J. S.; Epstein, A. J. Adv Mater 2002, 14, 1230.
- Miller, J. S.; Epstein, A. J. Chem Commun 1998, 1319.
- Haskel, D.; Islam, Z.; Lang, J.; Kmety, C.; Srajer, G.; Pokhodnya, K. I.; Epstein, A. J.; Miller, J. S. Phys Rev B 2004, 70, 054422.

10. Her, J.-H.; Stephens, P. W.; Pokhodnya, K. I.; Bonner, M.; Miller, J. S. *Angew Chem Int Ed* 2007, 46, 1521.
11. Dronskowski, R. *Computational Chemistry of Solid State Materials*. Wiley-VCH: New York, 2005.
12. Liu, X.; Krott, M.; Müller, P.; Hu, C.; Lueken, H.; Dronskowski, R. *Inorg Chem* 2005, 44, 3001.
13. Krott, M.; Liu, X.; Fokwa, B. P. T.; Lueken, H.; Dronskowski, R. *Inorg Chem* 2007, 46, 2204.
14. Kresse, G.; Furthmüller, J. *VASP the Guide*. Institut für Materialphysik, Universität Wien, 2007.
15. Dudarev, S. L.; Botton, G. A.; Savrasov, S. Y.; Humphreys, C. J.; Sutton, A. P. *Phys Rev B* 1998, 57, 1505.
16. Di Sipio, L.; Tondello, E.; De Michelis, G.; Oleari, L. *Chem Phys Lett* 1971, 11, 287.
17. Tchougréeff, A. L.; Misurkin, I. A. *Phys Rev B* 1992, 46, 5357.
18. Tchougréeff, A. L. *J Chem Phys* 1992, 96, 6026.
19. Hoffmann, R. *Solids and Surfaces: A Chemist's View of Bonding in Extended Structures*; VCH: New York, 1988.
20. Ashcroft, N. W.; Mermin, N. D. *Solid State Physics*; Holt, Rinehart & Winston. NY et al. 1976; chapter 28, eqs. (28.17), (28.20).